An improved sliding mode control combined with backstepping techniques and artificial neural networks for a coupled-tank system

Huynh Dac Son Tien, Phan Nhut Tan, Pham Thanh Tung*

Vinh Long University of Technology Education, 73 Nguyen Hue, Long Chau, Vinh Long, Vietnam.
*Corresponding author: tungpt@vlute.edu.vn
Received 28 Dec. 2025; Revised 16 Apr. 2026; Accepted 15 Jun. 2026; Published 25 Jun. 2026.
DOI: https://doi.org/10.54939/1859-1043.j.mst.112.2026.20-28

ABSTRACT

This study proposes a solution to design a liquid level tracking controller for a coupled-tank system (C-TS) using a sliding mode control (SMC) method based on proportional integral (PI) sliding surface (SS) combined with backstepping techniques and radial basis function neural networks (RBFNNs). The SMC controller based on proportional integral sliding surface (also called PISMC) provides more parameters with which to tune the SMC controller. The backstepping approach ensures the global asymptotic stability of strict feedback systems. The improved backstepping sliding mode control is employed to enhance the performance of conventional sliding mode control and act as a robust control strategy. The RBFNNs are utilized to approximate the unknown nonlinear functions in the improved backstepping sliding mode control. System stability is proven through Lyapunov theory. Simulation results in MATLAB/Simulink demonstrate the effectiveness, appropriateness, and robustness of the proposed control method in comparison with the fuzzy controller, adaptive control using RBF neural network, sliding mode control (SMC) based on disturbance observer and Quasi mode and sliding mode control using conditional integrators with the rising time achieves 0.1295 (s), the settling time is 0.2233 (s), the percent overshoot is 0 (%), the steady state error converges to zero.

Keywords: Coupled-tank system; Sliding mode control; Backstepping; Radial basis function neural networks; MATLAB/Simulink.

1. INTRODUCTION

Controlling the liquid level in tank systems holds critical importance across industries like petrochemicals, chemicals, pharmaceuticals, food processing [1, 2], wastewater management, water filtration systems, nuclear power plants, and automated fluid distribution networks [3]. These operations often involve pumping fluids into storage tanks and transferring them to other tanks as part of the process. A key physical constraint in these systems is the height of the tanks, which needs to be carefully managed to avoid overflow and reduce risks within the plant environment [4, 5].

Over the years, various control strategies have been researched and proposed for this system, including PI, PID, and Fuzzy controllers [1], MRAC (Model Reference Adaptive Control) compared with PI controller [2], adaptive control using RBF neural network [5], sliding mode control (SMC) based on disturbance observer and Quasi mode [6], addressing limitations of PI controllers [7], PID-Fuzzy controller designed using ANFIS system [8, 9], and higher-order SMC method, which have been benchmarked against conventional SMC approaches [10].

The objective of this study is to design a sliding mode controller with an improved sliding surface (also referred to as a proportional integral (PI) sliding surface) combined with backstepping techniques and RBFNNs to achieve finite-time liquid level tracking in a coupled-tank system (C-TS) while overcoming the chattering phenomenon inherent in classical SMC. The SMC has emerged as an effective tool to handle uncertainties and external disturbances in practical systems and is recognized as one of the robust feedback control methodologies [8]. The backstepping technique decomposes high-order complex control problems into a series of lower-order control

tasks via a recursive procedure, allowing for greater design flexibility and reducing system complexity constraints compared to other methods [9]. The RBFNNs structured with three layers: input, hidden, and output [11]. This network provides excellent approximation capabilities with global optimization potential [12, 13], a simple structure and fast learning ability [12, 14, 15].

This paper is structured as follows: Section 2 presents the controller design methodology; Section 3 displays the simulation results and discussions; conclusions are shown in Section 4.

2. CONTROLLER DESIGN

2.1. Mathematical model of the coupled-tank system

The mathematical model of the C-TS is illustrated in Figure 1 [1] with h_1 (*cm*) be the liquid level in Tank 1; h_2 (*cm*) be the liquid level in Tank 2; q_{in} (cm^3/min) be the inlet flow rate into Tank 1; q_1 (cm^3/min) be the outflow rate from Tank 1; q_o (cm^3/min) be the outflow rate from Tank 2; A_1 *(cm²)* and A_2 *(cm²)* be the cross-sectional areas of Tank 1 and Tank 2, respectively*;* R_1 and R_2 *(s/m²)* be the flow resistances of Tank 1 and Tank 2, respectively.

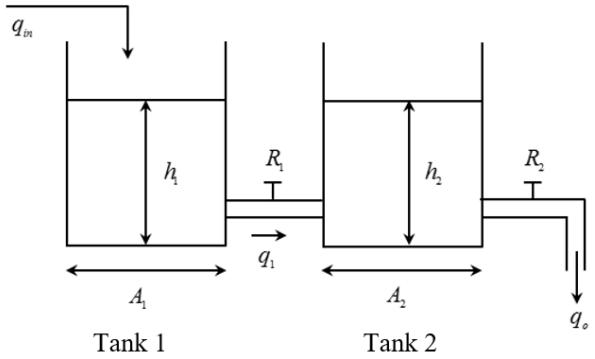

Figure 1. *Coupled-tank system model [1].*

We get (1) from Tank 1 [1]: $$A_1 \frac{dh_1}{dt} = q_{in} - q_1 \tag{1}$$

Considering a linear flow resistance:

$$q_1 = \frac{h_1 - h_2}{R_1} \tag{2}$$

$$A_1 \frac{dh_1}{dt} = q_{in} - \left(\frac{h_1 - h_2}{R_1} \right) \tag{3}$$

$$A_1 R_1 \frac{dh_1}{dt} = R_1 q_{in} - h_1 + h_2 \tag{4}$$

Tank 1's time constant as (5): $$\Omega_1 = A_1 R_1 \tag{5}$$

We have (6): $$\Omega_1 \frac{dh_1}{dt} + h_1 - h_2 = R_1 q_{in} \tag{6}$$

Taking the Laplace transform of (6), we get (7): $h_1(s) = \frac{R_1 q_{in}(s)}{\Omega_1 s + 1} + \frac{h_2(s)}{\Omega_1 s + 1}$ (7)

Similar to above, the following expression is obtained for Tank 2:

$$R_1 \Omega_2 \frac{dh_2}{dt} + h_2 R_2 + h_2 R_1 = h_1 R_2 \tag{8}$$

where $A_2 \frac{dh_2}{dt} = q_1 - q_0$, $q_0 = \frac{h_2}{R_2}$, $\Omega_2 = A_2 R_2$

Taking the Laplace transform of both sides of (8), we have (9):

$$\left(R_1\Omega_2 s + R_2 + R_1\right)h_2(s) = R_2 h_1(s) \tag{9}$$

Substituting (7) into (9), we get (10):

$$\left(\Omega_1\Omega_2 s^2 + \left(\Omega_1 + \Omega_2 + A_1R_2\right)s + 1\right)h_2(s) = R_2 q_{in}(s) \tag{10}$$

The transfer function of the C-TS is derived as follows (11) [1]:

$$G(s) = \frac{h_2(s)}{q_{in}(s)} = \frac{\eta}{\mu s^2 + \beta s + 1} \tag{11}$$

where $\eta = R_2; \mu = \Omega_1\Omega_2; \beta = \Omega_1 + \Omega_2 + A_1R_2$

Taking the inverse Laplace transform, we obtain: $\ddot{y}(t) + \frac{\beta}{\mu}\dot{y}(t) + \frac{1}{\mu}y(t) = \frac{\eta}{\mu}u(t)$ (12)

where $h_2(t) = y(t)$ is the output, and $q_{in}(t) = u(t)$ is the input of the system.

The state-space model of the C-TS is given by (13):

$$\begin{cases} \dot{z}_1(t) = z_2(t) \\ \dot{z}_2(t) = \xi(z) + \frac{\eta}{\mu}u(t) \\ y(t) = z_1(t) \end{cases} \tag{13}$$

where $z_1(t) = h_2(t) = y(t)$ and $z_2(t) = \dot{z}_1(t) = \dot{h}_2(t)$ are the state variables, $\xi(z) = -\frac{1}{\mu}z_1(t) - \frac{\beta}{\mu}z_2(t)$. The control objective is to regulate the liquid level in Tank 2 (h_2) to a reference level. The C-TS is transformed into a strict-feedback form to facilitate the backstepping control design. The unknown nonlinear functions correspond to the nonlinear flow dynamics and interconnection terms between the tanks, which are approximated using RBF neural networks.

2.2. Proportional integral backstepping sliding mode control

In this section, the proportional integral SMC controller combined with backstepping technique (BSMCPI) based on the exponential reaching law (ERL) for the C-TS is presented. The proposed controller incorporates an improved proportional–integral (PI) sliding surface into the backstepping framework to improve steady-state performance and enhance tracking accuracy. The fundamental design steps of the BSMCPI-ERL controller are as follows:

Step 1

Define the tracking error as (14): $e_r(t) = y(t) - h_{2d}(t) = z_1(t) - h_{2d}(t)$ (14)

where $h_{2d}(t)$ denotes the desired liquid level in Tank 2.

Taking derivative on both sides (14), we obtain (15):

$$\dot{e}_r(t) = \dot{z}_1(t) - \dot{h}_{2d}(t) = z_2(t) - \dot{h}_{2d}(t) \tag{15}$$

The Lyapunov function is defined as (16): $L_1(t) = \frac{1}{2}e_r^2(t)$ (16)

Taking derivative of (16), we obtain (17): $\dot{L}_1(t) = e_r(t)\dot{e}_r(t) = e_r(t)\left(z_2(t) - \dot{h}_{2d}(t)\right)$ (17)

In order to $\dot{L}_1(t) \le 0$, we choose $z_2(t) = \sigma(t) - \dot{e}_r(t) - (\lambda + 2\alpha)e_r(t) - \alpha^2 \int_0^t e_r(\tau)d\tau + \dot{h}_{2d}(t)$,

which means that [16]: $\sigma(t) = 2\dot{e}_r(t) + (\lambda + 2\alpha)e_r(t) + \alpha^2 \int_0^t e_r(\tau)d\tau$ (18)

where $\alpha > 0, \lambda > 0$, $\sigma(t)$ is the sliding surface.

Substituting (18) into (17), we obtain:

$$\dot{L}_1 = \frac{1}{2}\left(e_r(t)\sigma(t) - (\lambda + 2\alpha)e_r^2(t) - \alpha^2 \int_0^t e_r^2(\tau)d\tau \right) \quad (19)$$

If $\sigma(t) = 0$ then $\dot{L}_1(t) \le 0$. Therefore, Step 2 will be carried out.

Step 2

The Lyapunov function is defined as follows: $L_2(t) = L_1(t) + \frac{1}{2}\sigma^2(t)$ (20)

Because $\dot{\sigma}(t) = \dot{z}_2(t) - \ddot{h}_{2d}(t) + \ddot{e}_r(t) + (\lambda + 2\alpha)\dot{e}_r(t) + \alpha^2 e_r(t)$

Thus, we have:

$$\begin{aligned} \dot{L}_2(t) &= \dot{L}_1(t) + \sigma(t)\dot{\sigma}(t) \\ &= -\left((\lambda + 2\alpha)e_r^2(t) + \alpha^2 \int_0^t e_r^2(\tau)d\tau \right) + \sigma(t)\begin{pmatrix} \xi(z) + \frac{\eta}{\mu}u(t) + d(t) - \ddot{h}_{2d}(t) \\ + \ddot{e}_r(t) + \frac{1}{2}e_r(t) + (\lambda + 2\alpha)\dot{e}_r(t) + \alpha^2 e_r(t) \end{pmatrix} \end{aligned} \quad (21)$$

To ensure $\dot{L}_2(t) \le 0$, the PI backstepping sliding mode controller based on the exponential reaching law $\left(u_{BSMCPI-ERL}(t)\right)$ is designed as follows (22):

$$u_{BSMCPI-ERL}(t) = \frac{\mu}{\eta}\begin{pmatrix} -\xi(z) + \ddot{h}_{2d}(t) - \ddot{e}_r(t) - (\lambda + 2\alpha)\dot{e}_r(t) - \alpha^2 e_r(t) - \cdots \\ - c\sigma(t) - \frac{1}{2}e_r(t) - \delta sign\left(\sigma(t)\right) - \kappa\sigma(t) \end{pmatrix} \quad (22)$$

where $c > 0$, $\delta > 0$ $\kappa > 0$. Now, we have:

$$\dot{L}_2(t) = -(\lambda + 2\alpha)e_r^2(t) - \alpha^2 \int_0^t e_r^2(\tau)d\tau - c\sigma^2(t) - \kappa\sigma^2(t) - \delta\left|\sigma(t)\right| \le 0 \quad (23)$$

Thus, $e_r(t) \to 0$ when $t \to \infty$.

2.3. Application of RBF neural networks

In this section, the RBFNNs is utilized to approximate $\xi(z)$ in the control law (22). The algorithm of the RBFNNs is described as (24) and (25) [17, 18].

$$h_j = \exp\left(-\frac{\left\| z - c_j \right\|^2}{2b_j^2} \right) \quad (24)$$

$$\xi = \boldsymbol{W}^{*T}\boldsymbol{h}(z) + \varepsilon \tag{25}$$

The output of the RBFNNs is given by (26): $\hat{\xi}(z) = \hat{\boldsymbol{W}}^{T}\boldsymbol{h}(z)$ (26)

After the function $\xi(z)$ is approximated by the RBFNNs, the BSMCPIRBF controller is designed as follows (27):

$$u_{BSMCPIRBF}(t) = \frac{\mu}{\eta}\begin{pmatrix} -\hat{\xi}(z) + \ddot{h}_{2d}(t) - \ddot{e}_r(t) - (\lambda + 2\alpha)\dot{e}_r(t) - \alpha^2 e_r(t) - \cdots \\ -c\sigma(t) - \frac{1}{2}e_r(t) - \delta sign(\sigma(t)) - \kappa\sigma(t) \end{pmatrix} \tag{27}$$

To prove stability, assumption that the required function approximates in the C-TS is assumed to belong to a compact set and can be approximated by RBFNNs with a bounded approximation error. The optimal approximation error is assumed to be bounded by a positive constant, and this error is incorporated into the derivative of the Lyapunov function. Under appropriate selection of control gains, all signals in the closed-loop system are guaranteed to be uniformly ultimately bounded (UUB).

The Lyapunov function is defined as follows (28): $L = \frac{1}{2}\sigma^2 + \frac{1}{2\gamma}\tilde{\boldsymbol{W}}^{T}\tilde{\boldsymbol{W}}$ (28)

where $\gamma > 0$, $\tilde{\boldsymbol{W}} = \hat{\boldsymbol{W}} - \boldsymbol{W}^{*}$

Since, $\xi(z) - \hat{\xi}(z) = \boldsymbol{W}^{*T}\boldsymbol{h}(z) + \varepsilon - \hat{\boldsymbol{W}}^{T}\boldsymbol{h}(z) = -\tilde{\boldsymbol{W}}^{T}\boldsymbol{h}(z) + \varepsilon$

Then

$$\dot{L} = \sigma\dot{\sigma} + \frac{1}{\gamma}\tilde{\boldsymbol{W}}^{T}\dot{\hat{\boldsymbol{W}}} = \sigma\left(\lambda\dot{e}_r(t) + \ddot{h}_{2d}(t) + \xi(z) - \frac{\eta}{\mu}u(t)\right) + \frac{1}{\gamma}\tilde{\boldsymbol{W}}^{T}\dot{\hat{\boldsymbol{W}}} \tag{29}$$

Now, we get: $\dot{L} = \sigma\dot{\sigma} + \frac{1}{\gamma}\tilde{\boldsymbol{W}}^{T}\dot{\hat{\boldsymbol{W}}} = \varepsilon\sigma - \delta|\sigma| + \tilde{\boldsymbol{W}}^{T}\left(\frac{1}{\gamma}\dot{\hat{\boldsymbol{W}}} - \sigma\boldsymbol{h}(z)\right)$ (30)

The adaptive law is derived as (31): $\dot{\hat{\boldsymbol{W}}} = \gamma\sigma\boldsymbol{h}(z)$ (31)

If we choose: $\delta > |\varepsilon|_{max}$

Then $\dot{L} = \varepsilon\sigma - \delta|\sigma| \le 0$ (32)

3. RESULTS AND DISCUSSIONS

The simulation diagram of the proposed controller for the C-TS in MATLAB/Simulink is presented in **Figure** 2. The parameters of the C-TS are used in simulation as follows: $A_1 = 0.0145(m^2)$, $A_2 = 0.0145(m^2)$, $R_1 = 1478.57(\mathrm{s}/m^2)$ and $R_2 = 642.86(\mathrm{s}/m^2)$. The parameters of the BSMCPIRBF controller are presented as follows: $\delta = 15.5$, $\lambda = 31$, $\alpha = 37$, $c = 5$ and $\kappa = 5.03$. The response and tracking error results of the BSMCPIRBF controller with $h_{2d} = 55(cm)$ applied to the C-TS are presented in Figure 3. The position h_2 converges to h_{2d} with a steady-state error approaching zero, the rising time achieves 0.1295 s, the settling time is 0.2233 s, and the overshoot is 1.3077e-07%. The performance indices of the BSMCPIRBF controller are presented in Table 1 and compared with the fuzzy controller [1], adaptive control using radial basis function (RBF) neural network [5], sliding mode control (SMC) based on disturbance observer

and Quasi mode [6] and sliding mode control using conditional integrators [18]. The performance metrics in Table 1 demonstrates the improvement of the BSMCPIRBF controller over the methods implemented in [1, 5, 6, 18]. Additionally, the chattering phenomenon has been significantly reduced as shown in Figure 4. This demonstrates the suitability of the proposed method for application to the system.

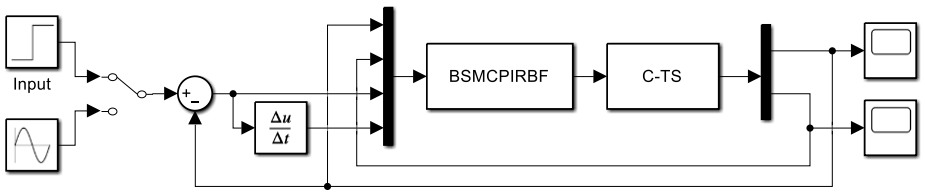

Figure 2. *Simulation diagram of the BSMCPIRBF controller.*

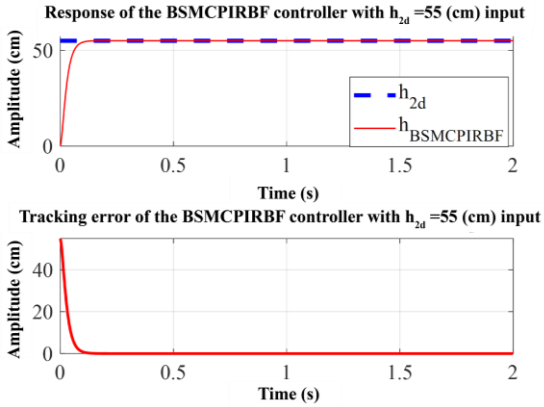

Figure 3. *Response and tracking error of the BSMCPIRBF controller with* $h_{2d} = 55(cm)$.

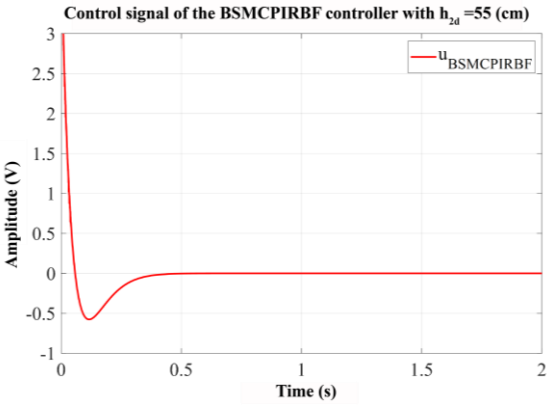

Figure 4. *Control signal of the BSMCPIRBF controller with* $h_{2d} = 55(cm)$.

Table 1. *Performance indices of the BSMCPIRBF controller.*

Metrics	**BSMCPIRBF**	**Fuzzy controller [1]**	**ASMCRBF [5]**	**SMC_DO_Q [6]**	**Sliding mode control using conditional integrators [18]**
Settling time (s)	0.2233	47.2	0.2464	0.5102	330
Rising time (s)	0.1295	33	0.1271	0.3183	87.184
Steady-state error (cm)	0	-	0	0	-
Overshoot ($\%$)	1.3077e-07	1.45	0	0	1.6

The response and error with square and sine wave inputs of the BSMCPIRBF controller are presented in Figures 5 and 6. Observing the signals in Figures 5 and 6, it is evident that the position of h_2 still converges to h_{2d} with in finite time, the steady-state error approaching zero. These results further confirms the validity and effectiveness of the proposed controller.

The responses with $h_{2d} = 55(cm)$, including step and sine wave signals of the BSMCPIRBF controller, are analyzed when the cross-sectional area constant of Tank 1 (A_1) is increased by 50%, as shown in Figure 7, that the steady-state error converging to zero.

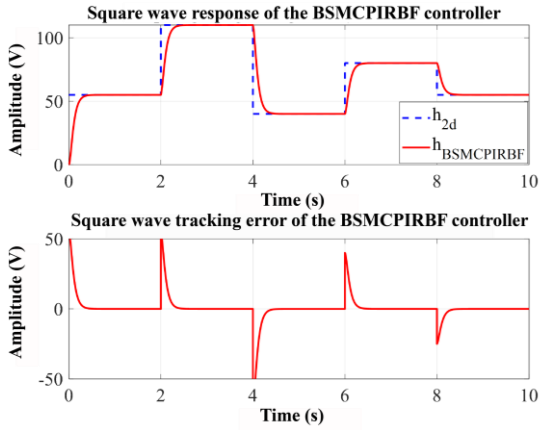

Figure 5. *Square signal response and error of the BSMCPIRBF controller.*

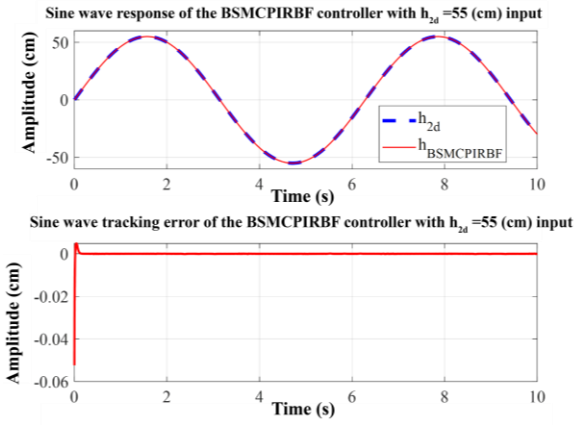

Figure 6. *Response and error of the BSMCPIRBF controller with sine signal.*

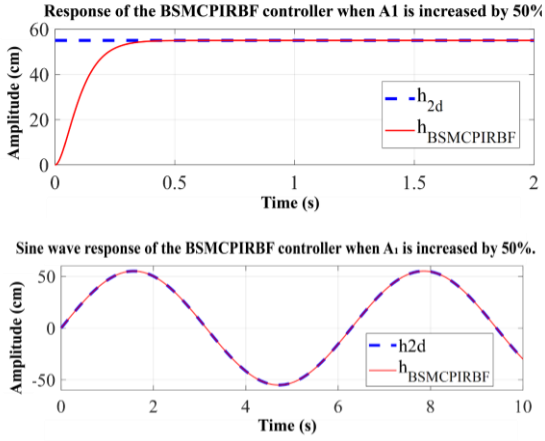

Figure 7. *Step and sine wave input responses* $h_{2d} = 55(cm)$ *of the BSMCPIRBF controller when the cross-sectional area* A_1 *is increased by 50%.*

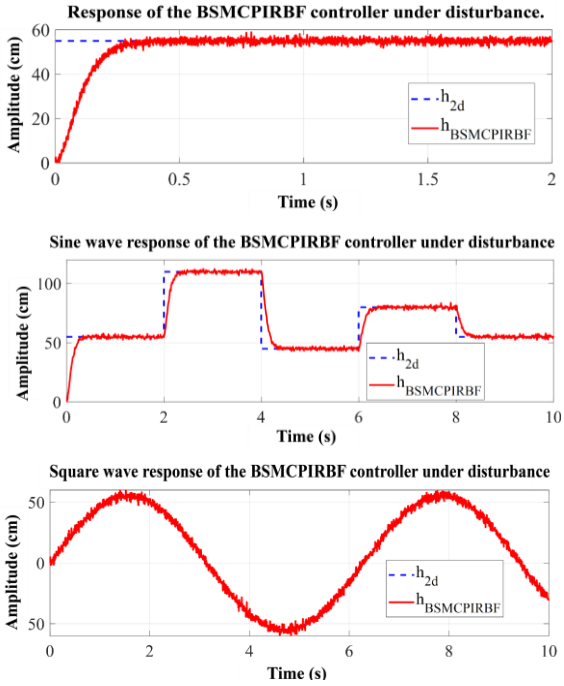

Figure 8. *Step, square wave, and sine wave input responses* $h_{2d} = 55(cm)$ *of the BSMCPIRBF controller under disturbance conditions.*

Figure 8 illustrates the system responses to step, square, and sine wave inputs $h_{2d} = 55(cm)$ of the proposed controller when subjected to external disturbances (white noise - assumed as sensor noise) with a power of 0.005 W applied at the system output. Observing the responses in Figure 8, it is evident that the actual position tracks the desired reference with in finite time. This result verifies the robustness of the proposed controller in position tracking control of the C-TS.

The results presented in Figures 3 to 8, along with the performance metrics summarized in Table 3, demonstrate that the BSMCPIRBF controller in this study effectively achieves accurate

liquid level tracking in the C-TS, eliminates chattering phenomena around the sliding surface, and maintains robustness against output disturbances.

4. CONCLUSIONS

This study presented the method to design the BSMCPIRBF controller for liquid level control in a C-TS. The proposed controller successfully achieved convergence to the desired liquid level in Tank 2 while reducing chattering effects C-TS and maintaining robustness against external disturbances and parameter uncertainties. Simulation results validate the controller's superior performance over the fuzzy controller, adaptive control using RBF neural network, sliding mode control (SMC) based on disturbance observer and Quasi mode and sliding mode control using conditional integrators. The controller demonstrates faster response times, zero steady-state error, and robustness under varying operating conditions. However, the results of this study are limited to simulations to evaluate the effectiveness of the proposed control method. Future research will focus on implementing the proposed controller in an experimental model and robustness tests under real disturbances to further validate its practical applicability.

REFERENCES

[1]. M. Changela and A. Kumar, "*Designing a Controller for Two Tank Interacting System,"* International Journal of Science and Research, Vol. 4, Issue 5, pp. 589 – 593, (2013).

[2]. M. Saad *et al.*, "*Performance Comparison between PI and MRAC for Coupled-Tank System,"* Journal of Automation and Control Engineering, Vol. 2, No. 3, pp. 316–321, (2014).

[3]. F. Zeng, "*A sufficient condition producing 16-qam golay complementary sequences,"* IEEE Communications Letters, Vol. 18, no. 11, pp. 1875–1878, (2014).

[4]. A. Yadav *et al.*, "*Sliding Mode Control with RBF Neural Network for Two Link Robot Manipulator,*"International Journal of Computer Applications, Vol. 178, No. 52, pp. 31 – 36, (2019).

[5]. P. T. Tung and N. C. Ngon, "*Adaptive sliding mode control based on RBF neural network for two tanks interacting system,"* TNU Journal of Science and Technology, Vol. 226, No. 11, pp. 323–331, (2021).

[6]. P. T. Tung and N. C. Ngon, "*Sliding mode control based on disturbance observer and Quasi-sliding mode for two_tank interacting system,"* TNU Journal of Science and Technology, Vol. 227, No. 02, pp. 87–95, (2022).

[7]. Sains and Kej, "*Intergral time absoluts error minimization for PI controller on coupled-tank liquid level control system based on stochastic search techniques,"* Faculty of Electrical Engineering, Universiti Teknologi Malaysia, Vol. 54, pp. 316–321, (2011).

[8]. S. N. Engin *et al.*, "*Modeling of a Coupled Industrial Tank System with ANFIS,"* Springer-Verlag Berlin Heidelberg, Vol. 2972, pp. 804-812, (2004).

[9]. D. Mursyitah *et al.*, "*Level Control in Coupled Tank System Using PID-Fuzzy Tuner Controller,*" 2018 Electr. Power, Electron. Commun. Control. Informatics Semin. EECCIS 2018, pp. 293–298, (2018).

[10]. K. Narwekar and V. A. Shah, "*Level control of coupled tank using higher order sliding mode control,"* Proc. 2017 IEEE Int. Conf. Intell. Tech. Control. Optim. Signal Process. INCOS 2017, Vol. 2018, No. 1, pp. 1–5, (2017).

[11]. Jinkun Liu, "*Radial basis function (RBF) neural network control for mechanical systems,"* Springer-Verlag Berlin Heidelberg, (2013).

[12]. M. A. M. Basri, "*Design and application of an adaptive backstepping sliding mode controller for a six-DOF quadrotor aerial robot,"* Robotica, Vol. 36, No. 11, pp. 1680–1700, (2018).

[13]. Y. Tao *et al.*, "*A Sliding Mode Control-Based on a RBF Neural Network for Deburring Industry Robotic Systems,"* International Journal of Advanced Robotic Systems, Vol. 13, No. 8, pp. 1-10, (2016).

[14]. Z. A. Khan *et al.*, "*RBF neural network based backstepping terminal sliding mode MPPT control technique for PV system*," PLoS ONE, Vol. 16, No. 4, pp. 1-23, (2021).

[15]. H. Zhang and Y. Liu, "*Adaptive RBF neural network based on sliding mode controller for active power filter*," Int. J. Power Electronics, 2020. Vol. 11, No. 4, pp. 460-481, (2020).

[16]. C. H. Lin and F.-Y. Hsiao, "*Proportional-Integral Sliding Mode Control with an Application in the Balance Control of a Two-Wheel Vehicle System,"* Applied Sciences, Vol. 10, No. 15, pp. 1-27, (2020).

[17]. L. Xu *et al.*, "*A combined backstepping and fractional-order PID controller to trajectory tracking of mobile robots,"* Systems Science and Control Engineering, Vol. 10, No. 1, pp. 133–140, (2022).

[18]. S. B. Prusty *et al*., "*Sliding Mode Control of Coupled Tank Systems Using Conditional Integrators,"* IEEE/CAA Journal of Automatica Sinica, Vol. 7, No. 1, pp. 118-125, (2020).

TÓM TẮT

Điều khiển trượt cải tiến kết hợp với kỹ thuật cuốn chiếu và mạng nơ-ron nhân tạo cho hệ thống bồn kép

Nghiên cứu này đề xuất một giải pháp thiết kế bộ điều khiển bám mức chất lỏng cho hệ thống bồn kép (C-TS) sử dụng phương pháp điều khiển trượt (SMC) dựa trên mặt trượt tích phân tỷ lệ (PI) kết hợp với kỹ thuật cuốn chiếu và mạng nơ-ron hàm cơ sở xuyên tâm (RBFNNs). Bộ điều khiển trượt dựa trên mặt trượt tích phân tỷ lệ (còn gọi là điều khiển trượt cải tiến - PISMC) cung cấp nhiều tham số hơn để điều chỉnh bộ điều khiển trượt. Phương pháp cuốn chiếu đảm bảo tính ổn định tiệm cận toàn cục của các hệ thống hồi tiếp nghiêm ngặt. Điều khiển trượt cuốn chiếu cải tiến được sử dụng để nâng cao hiệu suất của điều khiển trượt truyền thống và hoạt động như một chiến lược điều khiển bền vững. Mạng RBFNNs được sử dụng để xấp xỉ các hàm phi tuyến chưa biết trong điều khiển trượt cuốn chiếu cải tiến. Tính ổn định của hệ thống được chứng minh thông qua lý thuyết Lyapunov. Kết quả mô phỏng trong MATLAB/Simulink chứng minh tính hiệu quả, sự phù hợp và tính bền vững của phương pháp điều khiển đề xuất so với điều khiển mờ, điều khiển thích nghi sử dụng mạng nơ-ron RBF, điều khiển trượt dựa vào quan sát nhiễu và chế độ Quasi và điều khiển trượt dựa vào các điều kiện tích phân, với thời gian tăng đạt 0,1295 (s), thời gian xác lập là 0,2233 (s), không có vọt lố và sai số xác lập hội tụ về 0.

Từ khoá: Hệ thống bồn đôi; Điều khiển trượt; Cuốn chiếu; Mạng nơ-ron hàm cơ sở xuyên tâm; MATLAB/Simulink.